Multichannel wavelength multicasting for two QPSK signals based on FWM in SOA

Jun Qin (秦 军)[1], Yuefeng Ji (纪越峰)[1*], Hongxiang Wang (王宏祥)[1], Danshi Wang (王丹石)[1], Min Zhang (张 民)[1], and Guo-Wei Lu (吕国伟)[2]

[1]*State Key Laboratory of Information Photonics and Optical Communication, School of Information and Communication Engineering, Beijing University of Posts and Telecommunications, Beijing 100876, China*

[2]*Institute of Innovative Science and Technology, Tokai University, Japan*

[*]*Corresponding author: jyf@bupt.edu.cn*

Received August 22, 2014; accepted October 24, 2014; posted online December 12, 2014

We experimentally demonstrate multichannel wavelength multicasting for two nonreturn-to-zero quadrature phase-shift keying (NRZ-QPSK) channels based on four-wave mixing (FWM) in semiconductor optical amplifier (SOA). Through the interaction with the two pumps in SOA, the input two 25 Gb/s NRZ-QPSK channels are successfully simultaneously multicast to five and two new wavelengths, respectively. All the multicast channels are with a power penalty less than 2.5 dB at a bit error rate (BER) of 10^{-3}. A characterization of the system performance using conversion efficiency and BER as figures-of-merit in terms of pump and signal powers is also presented. The results indicate that the pump and signal powers can be optimized to eliminate the introduced deleterious nonlinear components. The wavelengths of the two NRZ-QPSK channels and the two pumps need to be specified to avoid the crosstalk induced by high-order FWM.

OCIS codes: 060.2330, 060.4255, 190.4380.

doi: 10.3788/COL201513.010601.

Optical wavelength multicasting, which can efficiently send a stream of information carried by one input wavelength to a number of different wavelengths has been regarded as an essential and important functionality in the next generation all-optical transparent networks. With the multicasting technology, the data of the new emerging applications such as streaming media or high-definition television can be easily delivered from one server side to the users' sides that employ different wavelengths. Today in the optical networks, migration operation between data centers which needs to transfer huge amounts of user data from one data center to other data centers is another challenging issue. The multicasting technology can be an efficient way to solve the problem, by adjusting the output channel numbers and wavelength of the multicasting scheme, the migration operation can be more efficient and flexible. To the whole optical network, by employing the multicasting technology, the network efficiency and throughput can be improved effectively[1], and with an all-optical way, the cost and energy consumption can be reduced significantly compared with the traditional electronic way.

During the past decade, various wavelength multicasting schemes have been extensively studied and demonstrated in different nonlinear devices, including highly nonlinear fiber[2–6] and silicon waveguide[7]. But these works mainly involved with intensity modulated nonreturn-to-zero on–off-keying (NRZ-OOK), return-to-zero (RZ) OOK, and differential phase-shift-keying signals, and most of these schemes suffer from drawbacks such as relatively high input powers, poor conversion efficiency (CE), and complicated system architecture. With periodically poled lithium niobate (PPLN) waveguide, multicasting for 16 quadrature amplitude modulation (QAM) signal has been reported in Ref. [8], but due to the high damage power threshold of PPLN, less number of output multicast wavelengths were achieved.

With the ever-growing internet traffic, high spectral efficiency phase-modulated signals have attracted interest for use in long-haul, high-capacity wavelength-division multiplexing WDM systems[9]. Quadrature phase-shift keying (QPSK) is an attractive data modulation format, by multilevel data encoding, its symbol rate is half the bit rate on the transmission line facilitating the improvement of the spectral efficiency. The multicasting of QPSK signal will have more practical significance for the reason that it has been used as standard in the commercial 100 Gb/s Ethernet system. Semiconductor optical amplifier (SOA), as an important nonlinear device in optical signal processing, offers advantages in terms of low-optical power consumption and relatively high CE[10] compared with other nonlinear mediums. In addition, the use of SOAs allows the integration of multicasting with other components, such as lasers and switches. The constant amplitude envelope of the QPSK signal would make it possible to use SOA-based multicasting without the degrading effects of cross-gain modulation. Four-wave mixing (FWM) in SOA has been proposed for wavelength multicasting as an efficient way[11]. Contestabile *et al.*[11] demonstrated a scheme for multicasting an input signal to six output wavelengths by employing three pumps with different states of polarizations. However, the scheme suffers complexity in controlling the polarization state, low

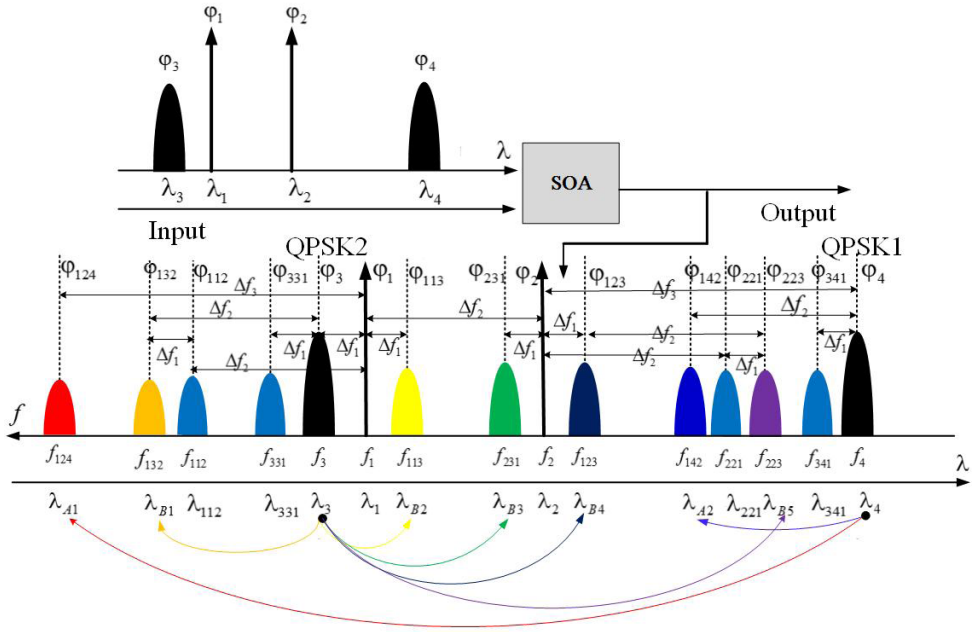

Fig. 1. Operation principle of the MWM scheme for two QPSK channels wavelength multicasting based on FWM in SOA.

signal bit rate, and contraposing simply NRZ signal, and the results cannot be extended to phase-modulated signals in a straightforward way[12].

To the best of our knowledge, all the reported works of wavelength multicasting are aimed at transferring one input signal, named delivering the information carried by one input wavelength to several different output wavelengths, that is, single-channel wavelength multicasting (SWM). A loadable goal of the multicasting scheme could be simultaneously multicast multiple input signals, namely delivering the information carried by two or more input wavelengths that carry different data to different output wavelengths, that is, multichannel wavelength multicasting (MWM). By employing one MWM module, many SWM modules can be replaced, resulting in a smaller footprint and lower power consumption. With MWM scheme the capacity and flexibility of the optical network can be further improved. Matsuura *et al.*[13] demonstrated simultaneous four-channel wavelength conversion for NRZ-differential QPSK signal, but did not implement wavelength multicasting. In our previous work[14], we achieved SWM for QPSK signal, the input one 25 Gb/s NRZ-QPSK signal was successfully multicast to five new wavelengths with all information preserved. In this letter, we extend our previous work to MWM. We experimentally demonstrate simultaneous two NRZ-QPSK channels wavelength multicasting based on FWM in SOA. The input two 25 Gb/s NRZ-QPSK channels are successfully simultaneously multicast to five and two new wavelengths (one-to-five and one-to-two), respectively. The new generated channels exhibit relatively high optical signal-to-noise ratio (OSNR) and acceptable power penalty. Different from our previous work where only single input signal was multicasted, namely SWM, through FWM in SOA, here we present and experimentally demonstrate, to the best of our knowledge, the simultaneous multicasting of two input signals, that is, MWM, using single SOA device.

The proposed MWM scheme for two NRZ-QPSK channels is based on four-waves (two pump lights and two signal lights) FWM in SOA. Figure 1 schematically illustrates the principle of our two QPSK channels wavelength multicasting. As shown in Fig. 1, at the input side of the SOA are four FWM participators including two pump lights at wavelengths λ_1, λ_2 and two signal lights at λ_3 (QPSK2) and λ_4 (QPSK1). The corresponding frequencies of the four input lights are indicated by f_1–f_4. To effectively avoid crosstalk induced by high-order FWM, the spacing between the four lights is set to be unequal. As shown in Fig. 1, the spacing between the two pumps, pump λ_1 and signal λ_3, pump λ_2 and signal λ_4 are 500 GHz (Δf_2), 130 GHz (Δf_1), and 850 GHz (Δf_3), respectively. Although the spacing between the pumps and the signals are uneven, it is possible to ensure the new generated FWM idlers compliant with the ITU channels by setting the separations among the pumps and signals are multiples of 0.8 nm[15]. In a flexible grid network environment, the output multicast channels do not need to be constrained to compliant with the ITU channels, the optical network can be more flexible and elastic, and the setting of the spacing between the input signals can be more agile. After generation, these four waves are coupled together and are injected into the SOA. Both degenerate FWM (D-FWM) and non-degenerate FWM (ND-FWM) happen inside the SOA and some new frequencies are generated[16] (Fig. 1). Each of the generated component through D-FWM and ND-FWM possesses a frequency of $f_{abc}=f_a+f_b-f_c$ ($b\neq c$; a, b, and $c\in 1$, 2, 3, and 4), and a phase of

$\varphi_{abc}=\varphi_a+\varphi_b-\varphi_c$ ($b\neq c$; a, b, and $c\in 1, 2, 3$, and 4)[17,18]. When $a=b$, it is D-FWM component, whereas when $a\neq b$ it is ND-FWM component. But due to the low FWM efficiency, not all of the frequencies derived from $f_{abc}=f_a+f_b-f_c$ can be obtained. Figure 1 only presents the frequencies that we obtained in our experiment. The relationship of the electrical field (E) and the optical phase (φ) for the generated idlers at λ_{A1}–λ_{A2} (λ_{A1}–λ_{A2} are ND-FWMs) and λ_{B1}–λ_{B5} (λ_{B2} and λ_{B5} are D-FWMs and λ_{B1}, λ_{B3}, and λ_{B4} are ND-FWMs) can be expressed as[17]

$$E_{A1} \propto A_1 A_2 A_4^*, \quad \varphi_{A1} = \varphi_1 + \varphi_2 - \varphi_4, \tag{1}$$

$$E_{A2} \propto A_1 A_4 A_2^*, \quad \varphi_{A2} = \varphi_1 + \varphi_4 - \varphi_2, \tag{2}$$

$$E_{B1} \propto A_1 A_3 A_2^*, \quad \varphi_{B1} = \varphi_1 + \varphi_3 - \varphi_2, \tag{3}$$

$$E_{B2} \propto A_1^2 A_3^*, \quad \varphi_{B2} = 2\varphi_1 - \varphi_3, \tag{4}$$

$$E_{B3} \propto A_2 A_3 A_1^*, \quad \varphi_{B3} = \varphi_2 + \varphi_3 - \varphi_1, \tag{5}$$

$$E_{B4} \propto A_1 A_2 A_3^*, \quad \varphi_{B4} = \varphi_1 + \varphi_2 - \varphi_3, \tag{6}$$

$$E_{B5} \propto A_2^2 A_3^*, \quad \varphi_{B5} = 2\varphi_2 - \varphi_3, \tag{7}$$

where A_i, $i\in[1,2,3,4]$ is the field amplitude of the input lights and * represents the conjugate operation. Since the two pumps at λ_1 and λ_2 are not phase modulated (i.e., constant phase), it can be derived from Eqs. (1) to (7) that the original QPSK1 and QPSK2 signals at λ_4 and λ_3 will be transferred to λ_{A1}–λ_{A2} and λ_{B1}–λ_{B5}, respectively. All of the phase information of the original input two QPSK channels are effectively preserved in the new generated FWM components at λ_{A1}–λ_{A2} and λ_{B1}–λ_{B5}; therefore, MWM for two QPSK channels can be achieved.

Including the new generated idlers at λ_{A1}–λ_{A2} and λ_{B1}–λ_{B5}, some more frequencies can also be obtained. However, except the idlers at λ_{A1}–λ_{A2} and λ_{B1}–λ_{B5}, the other frequencies cannot preserve the information of the original input signal. The reasons include several aspects: 1) the absence of the original input QPSK signals in the FWM processes such as the generated frequency at λ_{112} ($\varphi_{112}=2\varphi_1-\varphi_1$) or λ_{221} ($\varphi_{221}=2\varphi_2-\varphi_1$) which are indicated by λ_{112} and λ_{221} in the optical spectra in Fig. 2. From the expression of the optical phase we can see that the light at λ_{112} or λ_{221} will carry no information because there is no original input QPSK signals' participation in the FWM processes. 2) The phase erasing characteristic of the FWM processes[19], taking the frequency at λ_{331} (indicated by λ_{331} in the optical spectra in Fig. 2), for example, the idler at λ_{331} which are generated by the interaction between signal f_3 and pump f_1. The phase modulation depth for the phase information at f_3 is doubled in the resultant phase pattern at λ_{331} ($\varphi_{331}=2\varphi_3-\varphi_1$). So, the information of the original QPSK2 signal cannot be preserved at λ_{331}, it can finally be encoded as binary phase-shift keying signal. 3) Both of the input two QPSK signals' participation in the FWM processes such as the idler at λ_{341} in Fig. 2. λ_{341} is generated by the FWM process between f_1, f_3, and f_4. The E and φ can be derived as $E_{341}\propto A_3 A_4 A_1^*$ and $\varphi_{341}=\varphi_3+\varphi_4-\varphi_1$, owing to the phase wrap characteristic with a periodicity of 2π, λ_{341} carries out modulo 4 operations of quaternary addition[20].

The relationship of the frequency interval of the new generated idlers with the spacing between the signals and the pumps are also shown in Fig. 1.

The experiment setup of our MWM scheme for two 25 Gb/s NRZ-QPSK channels wavelength multicasting in SOA is shown in Fig. 3(a). On the signal branch, two 25 Gb/s NRZ-QPSK signals are generated by the dual QPSK channel transmitter and then amplified by an erbium-doped fiber amplifier (EDFA). After the EDFA, an optical band-pass filter (OBPF) is used to filter out the out-of-band noise. On the pump branch, two pumps at λ_1 1544.13 nm and λ_2 1548.11 nm are generated by two tunable external cavity laser (ECL) and followed by polarization controller (PC) to adjust the polarization, EDFA to amplify the power and OBPF to remove the noise introduced by the EDFA. The two pumps are set co-polarized with each other by properly adjusting the PCs to reduce the system polarization sensitivity[21–24]. After generation, the pumps are coupled with the two QPSK signals into the SOA through a 3 dB coupler. The light sources of the input QPSK signals, the pumps and the local oscillator (LO) at the coherent receiver are all with narrow linewidth of 100 kHz to reduce the added phase noise. The SOA (CIP SOA-NL-OEC-1550) being used here is a commercially available device which has a small signal gain of 34 dB and a 6 dBm saturation output power operating over the C-band. The carrier recovery time of the SOA is typically 25 ps which does not cause any degradation to the multicast signals. In the experiment, the SOA is biased at 280 mA. At the output of the SOA, the new generated FWM terms are filtered by a one-to-nine Finisar wavelength selec-

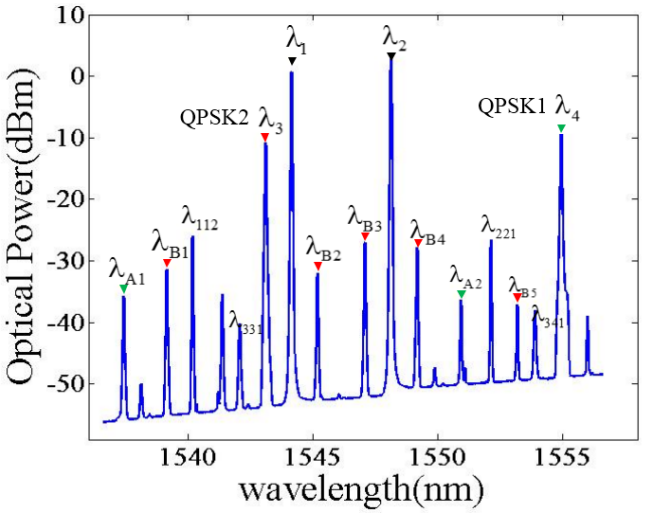

Fig. 3. Optical spectra at the output of the SOA.

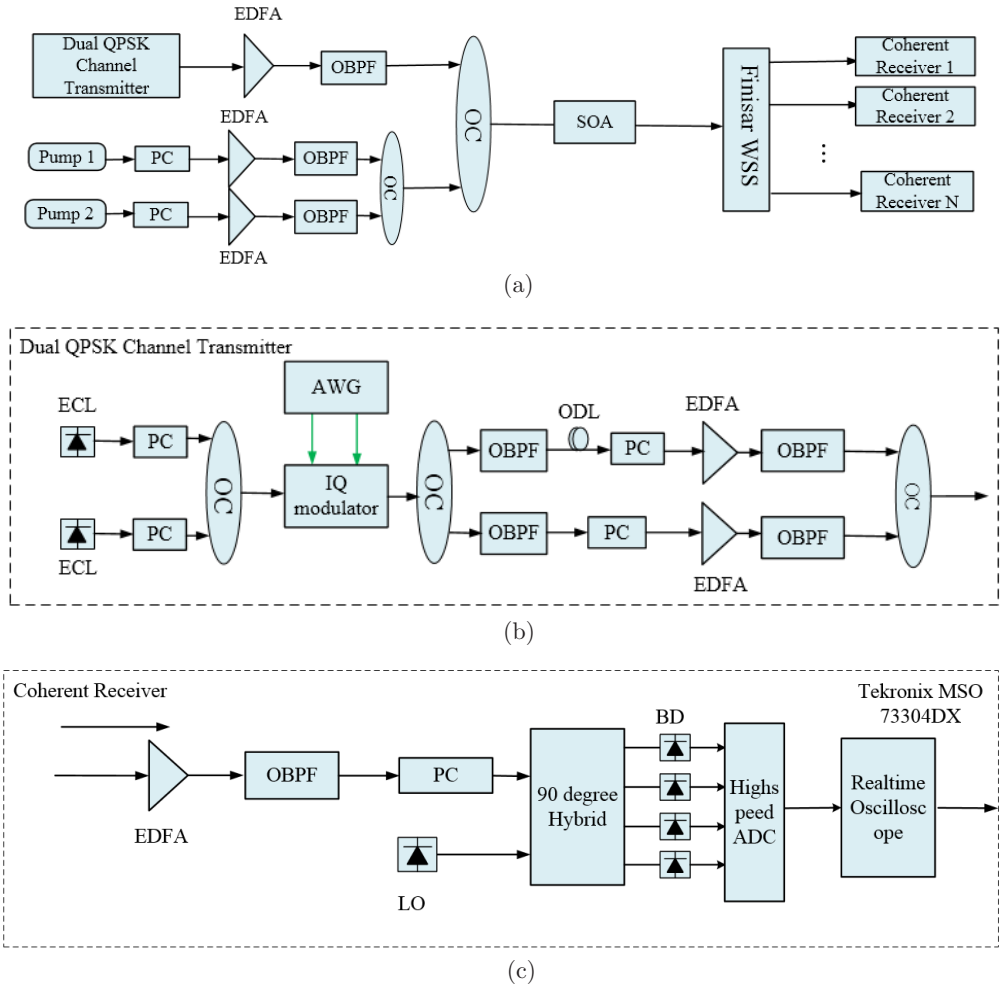

Fig. 3. Experiment setup of (a) two QPSK channels wavelength multicasting in SOA, (b) dual QPSK channel transmitter, and (c) coherent receiver. OC, optical coupler; BD, balanced detector; ADC, analog to digital converter.

tive switch (WSS) (Finisar DWPF, Flexgird) based on liquid crystals on silicon with variable bandwidths and then sent to a coherent receiver for detection.

The detailed setup of the dual QPSK channel transmitter is shown in Fig. 3(b). Two continuous-wave lasers at λ_3 1543.09 nm and λ_4 1554.94 nm are coupled into an inphase/quadrature (IQ) modulator which has a 23 GHz 3 dB bandwidth and 5 V half-wave voltage to generate the NRZ-QPSK signal. Two de-correlated level 2 driving electronics originally from PRBS streams with length of 2^{15}–1 are generated from an arbitrary waveform generator (AWG) to drive the IQ modulator. After undergoing relative delay by optical delay line (ODL), polarization control, amplification, and filtering, the two QPSK signals can be coupled together through a coupler.

Figure 3(c) shows the structure of the coherent receiver. At the receiver, an EDFA is employed as pre-amplifier, after the EDFA an OBPF with a bandwidth of 0.4 nm is used to remove out-of-band amplified spontaneous emission noise. After pre-amplifying, the incoming signal will be sent into an optical 90° hybrid to interfere with the LO. Two balanced photo-detectors (BPDs) are used to detect the signal (OM4106D, Tektronix). The electrical signals after the BPDs are sampled by a real-time storage oscilloscope operating at 80 Gasa/s with 30 GHz electrical bandwidth (MSO 73304DX, Tektronix). The captured data are then off-line processed through digital signal processing.

Figure 2 shows the optical spectra measured at the output of the SOA, the two pump lights and the two NRZ-QPSK signal lights (QPSK1 and QPSK2) are indicated by λ_1, λ_2, λ_4, and λ_3, respectively. At the output of the SOA, as analyzed above, two new generated idlers can preserve the information of the original QPSK1 signal, denoted by λ_{A1}–λ_{A2} in Fig. 2. The five idlers which are denoted by λ_{B1}–λ_{B5} will keep the information of QPSK2. Among these seven idlers, the components at λ_{A1} is with conjugated phase compared with the input QPSK1 signal at λ_4. Similarly, the idlers at λ_{B2}, λ_{B4}, and λ_{B5} have phase conjugation with the original input QPSK2 signal at λ_3. Optical phase conjugation is one of the practical approaches to compensate for both chromatic dispersion and nonlinearity from long-haul transmission. The other idlers generated by the FWM process in the experiment are also shown in Fig. 2.

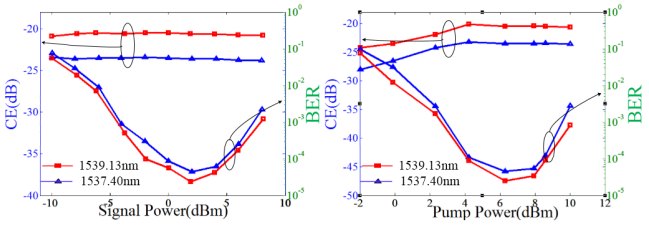

Fig. 4. Measured CE and BER when (a) tuning input signal power with fixed pump power and (b) tuning input pump power with fixed signal power.

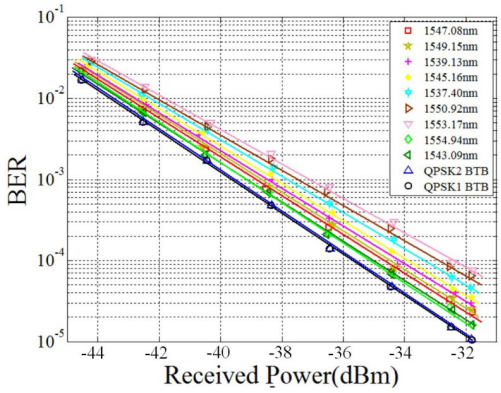

Fig. 5. Measured BER performance versus received power of the multicast channels.

However, they cannot carry the same information with the input signal, the reason has been presented earlier. With our current experimental setup, by changing the frequency spacing between the signals and pumps, the output multicasting channels can be consistent with the ITU channels.

Note that the frequency detuning of λ_1 to λ_2, λ_1 to λ_3, and λ_2 to λ_4 need to be adjusted properly to avoid frequency overlap for the new generated idlers. Frequency overlap will cause severe crosstalk[5,25].

To present the relationship between CE (defined as the ratio of the converted signal power to that of the input signal power) and input pumps power and signals power in SOA, we give a system characterization using CE and bit error rate (BER) as figures-of-merit in Fig. 4.

In Fig. 4(a), the power of the original input two QPSK signals increases from −11 to 8 dBm, whereas the input two pumps power are fixed at 6 dBm, the measured CE and BER for the multicast channels at λ_{A1} 1537.40 nm and λ_{B1} 1539.13 nm are depicted. When measuring the performance of the channel at λ_{A1}, the power of the input QPSK2 signal will be fixed. Similarly, when the channel at λ_{B1} is tested, the power of the input QPSK1 signal will be fixed. From the results we can see that the CE almost does not benefit from the increasing of the signal power, but when signal power is increasing it does help decrease the BER till around 2 dBm. When further increasing the signal power, the BER starts to increase which is probably caused by the self-phase modulation introduced distortions. Figure 4(b) shows the relationship of CE and BER as a function of the input pumps power. The pump power increases from −2 to 10 dBm, the power of the two QPSK signals can be fixed. Figure 4(b) shows that when increasing the pump power it does make contribution to the CE, therefore offering a sufficient OSNR for the converted signal resulting in a good BER performance. However, when the pump power is larger than 6 dBm, the added noise from high-order products introduced crosstalk can distort the performance resulting in increasing BER. Additionally, in-band crosstalk due to high-order FWM products can be particularly critical when the pump power is larger than 8 dBm. The best BER performances that can be achieved for the new generated idlers at λ_{A1} and λ_{B1} are 4.8×10^{-5} and 3.1×10^{-5}. The results of Fig. 4 indicate that not always with a high CE there will be a good BER performance but rather a compromise between the CE and the nonlinear noise. So, to eliminate the deleterious components in the converted signal, the powers of the pumps and signal shall be optimized. In our experiment, the optimal powers of the pump and signal are about 6 and 2 dBm, respectively. The average CEs of the two and five new multicast channels of QPSK1 and QPSK2 are −24.45 and −21.3 dB, respectively. To reduce the polarization sensitivity, orthogonal pumps scheme[21,26] and polarization diversity scheme with two independent circuits[27] can also be considered.

To further characterize the performance of the proposed two QPSK channels multicasting scheme, BER curves versus the received power for each multicast channel are measured and shown in Fig. 5. The powers of the each signal light and each pump light injected into the SOA are 2 and 6 dBm, respectively. The back-to-back (BTB) performance of the two input QPSK signals are also presented as a reference. The result in Fig. 5 indicates that at the BER of 10^{-3}, compared with the BTB case, the power penalty of the two multicast channels of QPSK1 at λ_{A1} and λ_{A2} is less than 2.0 dB. The five multicast channels of QPSK2 at λ_{B1}–λ_{B5} also exhibit small power penalty (from about 0.7 to less than 2.5 dB). The detailed performances including the CE and the power penalty at BER of 10^{-3} of the seven multicast channels are summarized in Table 1.

Table 1 indicates that the power penalty is sensitive to the CE which directly influences the OSNRs of the converted signal. For a relatively low CE at λ_{A1} and λ_{B5}, a small OSNR and large power penalty are measured.

Before the multicast signals were detected by the coherent receiver, we measured the spectral of the each wavelength at the output of the WSS (Figs. 6 and 7). The insets are the constellation and corresponding I/Q eye diagrams of the multicast QPSK signals after coherent detection and demodulation. The concentrated constellation and clear open eye prove the good quality of the multicast QPSK signal.

In conclusion, we discuss MWM for two NRZ-QPSK channels based on FWM in SOA. We experimentally

Table 1. Multicast Channel Performance

	Wavelength (nm)	Estimated OSNR (dB)	CE (dB)	Power Penalty (dB)
λ_{A1}	1537.40	18.5	−23.6	1.8
λ_{A2}	1550.92	14.3	−25.3	2.0
λ_{B1}	1539.13	22.2	−20.5	1.0
λ_{B2}	1545.16	19.8	−22	1.2
λ_{B3}	1547.08	24.4	−18	0.7
λ_{B4}	1549.15	22.8	−19.2	0.8
λ_{B5}	1553.17	14.1	−26.8	2.5

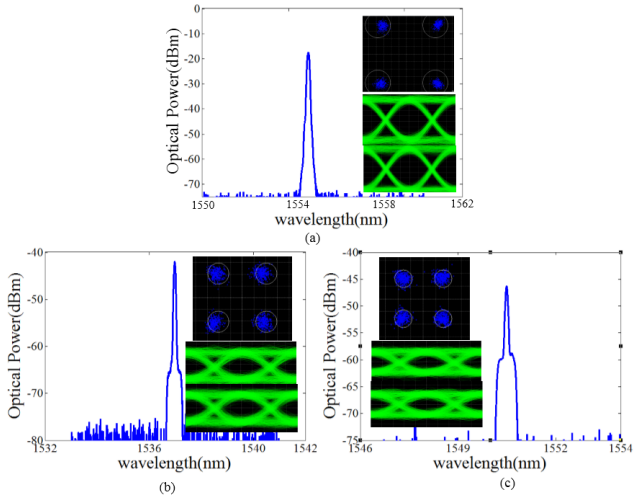

Fig. 6. Optical spectra of the multicast QPSK1 channels after the WSS at different wavelengths: (a) λ_4, 1554.94 nm; (b) λ_{A1}, 1537.40 nm; (c) λ_{A2}, 1550.92 nm. Insets: constellation and I/Q eye diagrams of the multicast signal on each wavelength.

demonstrate the one-to-five and one-to-two WDM multicasting for the input two 25 Gb/s NRZ-QPSK channels employing two pumps in SOA. The new generated QPSK channels are with a power penalty less than 2.0 and 2.5 dB at a BER of 10^{-3} for the input QPSK1 and QPSK2 channels, respectively. The respective constellation and eye diagram of the new generated multicast channels are presented. We also give a characterization of the system performance using CE and BER as figures-of-merit in terms of pump and signal powers. The results indicate that the pump and signal powers need to be carefully controlled to avoid the performance distortion introduced by nonlinear effects. The biggest constraints of this proof-of-concept experiment can be the unbalanced output multicast channels for the input two signals. A laudable goal of the MWM scheme shall have a balanced output channel number. However, due to the low CE, not all the FWM components derived from $f_{abc}=f_a+f_b-f_c$ ($b\neq c$; a, b, and $c\in$ 1, 2, 3, and 4) can be successfully achieved and detected. To obtain equal number of output multicast channels, we believe that additional system optimization is required. The channel spacing between the input signal lights and pump lights and the input power of signals and pumps shall be carefully calculated, and the polarization state also shall be carefully adjusted to avoid the frequency overlapping, reduce the influence of the high-order FWM components, and further raise the CE to offer a sufficient OSNR of the components derived from $f_{abc}=f_a+f_b-f_c$. In our future work, we will optimize the system parameters to get a balanced system performance.

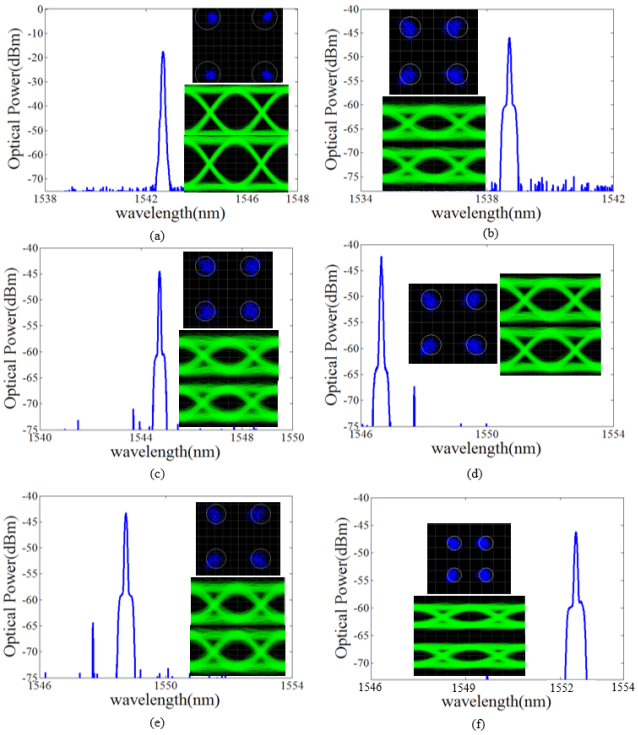

Fig. 7. Optical spectra of the multicast QPSK2 channels after the WSS at different wavelengths: (a) λ_3, 1543.09 nm; (b) λ_{B1}, 1539.13; (c) λ_{B2}, 1545.16; (d) λ_{B3}, 1547.08; (e) λ_{B4}, 1549.15; (f) λ_{B5}, 1553.17 nm. Insets: constellation and I/Q eye diagrams of the multicast signal on each wavelength.

This work was supported by the National 863 Program of China (Nos. 2012AA011302 and 2011AA010306) and the National Natural Science Foundation of China (No. 61372118).

References

1. G. N. Rouskas, IEEE Network **17,** 60 (2003).
2. C. S. Brès, A. O. Wiberg, B. Kuo, N. Alic, and S. Radic, IEEE Photon. Technol. Lett. **21,** 1002 (2009).
3. Z. Chen, L. Yan, W. Pan, B. Luo, A. Yi, Y. Guo, and J. H. Lee, IEEE Photon. Technol. Lett. **24,** 1882 (2012).
4. K. Inoue, T. Hasegawa, K. Oda, and H. Toba, Electron. Lett. **29,** 1708 (1993).
5. G. W. Lu, K. S. Abedin, and T. Miyazaki, Opt. Express **16,** 21964 (2008).
6. O. F. Yilmaz, S. R. Nuccio, X. Wang, J. Wang, I. Fazal, J. Y. Yang, X. Wu, and A. E. Willner, in *Proceedings of Optical Fiber Communication Conference* OWP8 (2010).
7. M. Pu, H. Hu, H. Ji, M. Galili, L. K. Oxenløwe, P. Jeppesen, J. M. Hvam, and K. Yvind, Opt. Express **19,** 2448 (2011).
8. A. Malacarne, G. Meloni, G. Berrettini, N. Sambo, L. Potì, and A. Bogoni, J. Lightw. Technol. **31,** 1797 (2013).
9. P. J. Winzer and R. J. Essiambre, J. Lightw. Technol. **24,** 4711 (2006).
10. A. Mecozzi, S. Scotti, A. D'ottavi, E. Iannone, and P. Spano, J. Quant. Electron. **31,** 689 (1995).
11. G. Contestabile, M. Presi, and E. Ciaramella, IEEE Photon. Technol. Lett. **16,** 1775 (2004).
12. B. Filion, W. Ng, A. T. Nguyen, L. A. Rusch, and S. LaRochelle, Opt. Express **21,** 19825 (2013).
13. M. Matsuura, N. Calabretta, O. Raz, and H. Dorren, Opt. Express **19,** B560 (2011).
14. J. Qin, H. Wang, D. Wang, M. Zhang, Y. Ji, and G.W. Lu, Chin. Opt. Lett. **12,** 110601 (2014).
15. K. Lau, L. Xu, S. Wang, L. Lui, P. Wai, C. Lu, and H. Tam, in *Proceedings of OECC/IOCC* (2007).
16. J. Hansryd, P. A. Andrekson, M. Westlund, J. Li, and P. O. Hedekvist, IEEE J. Sel. Top. Quant. Electron. **8,** 506 (2002).
17. N. Deng, K. Chan, C. K. Chan, and L. K. Chen, IEEE J. Sel. Top. Quant. Electron. **12,** 702 (2006).
18. G. W. Lu, K. S. Abedin, and T. Miyazaki, J. Lightw. Technol. **27,** 409 (2009).
19. G. W. Lu and T. Miyazaki, IEEE Photon. Technol. Lett. **21,** 322 (2009).
20. J. Wang, S. R. Nuccio, J. Y. Yang, X. Wu, A. Bogoni, and A. E. Willner, Opt. Lett. **37,** 1139 (2012).
21. G. Contestabile, L. Banchi, M. Presi, and E. Ciaramella, J. Lightw. Technol. **27,** 4256 (2009).
22. J. Ma, J. Yu, C. Yu, Z. Jia, X. Sang, Z. Zhou, T. Wang, and G. K. Chang, J. Lightw. Technol. **24,** 2851 (2006).
23. D. Wang, T. H. Cheng, Y. K. Yeo, Y. Wang,W. Zhao, J. Liu, and X. Gao, in *Proceedings of Optical Fiber Communication* (*OFC/NFOEC*) JWA47 (2010).
24. J. P. Lacey, M. A. Summerfield, and S. Madden, J. Lightw. Technol. **16,** 2419 (1998).
25. C. M. Gallep, H. J. S. Dorren, and O. Raz, IEEE Photon. Technol. Lett. **22,** 1550 (2010).
26. C. M. Gallep, O. Raz, and H. J. S. Dorren, in *Proceedings of Optical Fiber Communication* (*OFC/NFOEC*) OWP2 (2010).
27. G. Contestabile, A. D'Ottavi, F. Martelli, P. Spano, and J. Eckner, IEEE Photon. Technol. Lett. **14,** 666 (2002).